Published in final edited form as:
Nat Chem. 2021 August 01; 13(8): 805–810. doi:10.1038/s41557-021-00711-4.

Switching-on Prodrugs Using Radiotherapy

Jin Geng[#1,2,*], **Yichuan Zhang**[#1,2], **Quan Gao**[2], **Kevin Neumann**[1], **Hua Dong**[1], **Hamish Porter**[3], **Mark Potter**[4], **Hua Ren**[5,6], **David Argyle**[3], **Mark Bradley**[1,*]

[1]EaStCHEM School of Chemistry, University of Edinburgh, Edinburgh EH9 3FJ, United Kingdom

[2]Shenzhen Institute of Advanced Technology, Chinese Academy of Sciences, Shenzhen 518059, China

[3]The Royal (Dick) School of Veterinary Studies and Roslin Institute, University of Edinburgh, Easter Bush, Edinburgh EH25 9RG, United Kingdom

[4]Department of Surgery, Western General Hospital, Edinburgh EH4 2XU, United Kingdom

[5]Department of Radiation Oncology, National Cancer Center/National Clinical Research Center for Cancer/Cancer Hospital, Chinese Academy of Medical Sciences and Peking Union Medical College, Beijing 100021, China

[6]Department of Radiation Oncology, National Cancer Center/National Clinical Research Center for Cancer/Cancer Hospital & Shen Zhen Hospital, Chinese Academy of Medical Sciences and Peking Union Medical College, Shenzhen 518116, China

[#] These authors contributed equally to this work.

Abstract

Chemotherapy is a powerful tool in the armoury against cancer, however it is fraught with problems due to global systemic toxicity. Here we report the proof-of-concept of a chemistry-based strategy, whereby gamma/X-ray irradiation mediates the activation of a cancer prodrug thereby enabling simultaneous chemoradiotherapy with radiotherapy locally activating a prodrug. In an initial demonstration we show the activation of a fluorescent probe using this approach. Expanding on this, we show how sulfonyl azide and phenyl azide caged prodrugs of pazopanib and doxorubicin, can be liberated using clinically relevant doses of ionising radiation. This strategy is different to conventional chemo-radiotherapy radiation, where chemo-sensitization of the cancer takes place so that subsequent radiotherapy is more effective. This approach could enable site directed chemotherapy, rather than systemic chemotherapy, with “real time” drug decaging at the tumour site. As such it opens up a new era in targeted and directed chemotherapy.

[*] jin.geng@siat.ac.cn; mark.bradley@ed.ac.uk.

Author contributions

M.B. and J.G. conceived, designed, and directed the project. Y.Z., K.N., H.D. and H.P. conducted the compound synthesis, X-ray activation and characterisations. Y.Z. and J.G. conducted the MTT, flow cytometry, transwell and wound healing assays. Y.Z. and Q.G. conducted the *in vivo* experiments. J.G., Y.Z., M.P., H.R., D.A. and M.B. co-wrote the manuscript. All authors analysed the data and contributed to the scientific discussion and revised the manuscript.

Competing interests

The authors declare no competing interests.

Europe PMC Funders Author Manuscripts

Introduction

Many efforts have been made to improve the therapeutic index of anticancer agents. Chief amongst these is the prodrug approach with a proven clinical track record of improving administration routes, enhancing selectivities and reducing systemic toxicities.[1] The major therapeutically relevant routes to prodrug activation are typically *via* enzymes *e.g.* Capecitabine, which is an orally available form of 5-fluorouracil undergoes three enzymatic reactions *i.e.* carboxylesterase, Cyd deaminase and dThdPase in liver or/and tumours,[2] or physiological parameters such as pH *e.g.* Aldoxorubicin (INNO-206) which is an albumin-binding prodrug with release of doxorubicin under acidic conditions.[3–6] There are a number of prodrugs in the pipeline and in clinical trials. For instance, Apadaz™ releases its parent drug (hydrocodone) by enzymatic cleavage in the gastrointestinal tract.[7] Polyethylene glycol (PEG) "protected or blocked" interleukin-2 (IL-2) is a biologic prodrug with IL-2 liberated by *in vivo* release of the PEG chains.[8] Other, more academic prodrug stimuli have been explored in a variety of models, including electrochemical activation of metal-based prodrugs,[9] ultrasound-induced release,[10] or light mediated activation.[11]

Concurrent chemotherapy and radiation has been shown to give significantly better overall survival for the treatment of rectal,[12] lung[13] and breast[14] cancers than either alone. The combination of radiotherapy and hypoxia-activated prodrugs, such as evofosfamide and SN30000, (an analogue of tirapazamine) has also been reported.[15–17] However the combined toxicities of the dual treatments are often prohibitive necessitating a reduction in the intensity of either or both treatment modalities and a reduction in efficacy.

Linear accelerator technology for the precise delivery of radiotherapy allows the treatment of a variety of tumour types, including breast, lung, head and neck, prostate, gastrointestinal and gynaecological cancers.[18,19] Ionising radiation triggers a series of reactions in cells which generates a variety of reactive species such as free electrons, reactive oxygen species that include $O_2^{\bullet-}$, $^{\bullet}OH$ in the tumour area.[20,21] This gives rise to significant levels of DNA damage, including double-strand breaks,[22–28] which in turn leads to reaction with intercellular oxygen, and ultimately cell death. This may explain why hypoxic tissues/cancers are radiation resistant, in the absence of oxygen the DNA-derived free radicals are simply removed by glutathione.[29] Chemically it has been reported that gamma/X-rays can induce a variety of transformations,[30] thus reversible addition-fragment chain-transfer polymerisation can be initiated with gamma radiation.[31] Here we sought to develop a robust strategy to activate cancer prodrugs by the application of clinically relevant doses of gamma/X-ray irradiation (Figure 1). This strategy is totally different to conventional chemo-radiotherapy radiation, where chemo-sensitization of the cancer takes place so that subsequent radiotherapy is more effective and would allow site directed chemotherapy rather than systemic chemotherapy, allowing "real time" drug decaging at the tumour site *in vitro* and *in vivo* and opens up a new era in targeted and directed chemotherapy.

Results and Discussion

Chemical reactions under X-ray irradiation

A high-throughput screen was initially utilised to identify chemically relevant functional groups that were modified by gamma/X-ray irradiation – this included azides, disulfides, azobenzenes, triphenylphosphine, tetrazoles etc. with all reactions performed in an oxygen free environment in aqueous solution to mimic a hypoxic tumour environment (Table 1). We observed that molecules such as dipyridyl tetrazine and azobenzene did react under X-ray radiation (60 Gy), however, the resulting reaction mixtures were too complex to be useful (see Supplementary section). In the contrast, we also observed that a number of functional groups were converted cleanly and with high efficiency - thus 4-acetamidobenzenesulfonyl azide and some aromatic azides reacted under irradiation to give simple reaction mixtures that could be fully characterised.

As seen in Figure 2, 4-acetamidobenzenesulfonyl azide **1** (10 μM in PBS) gave rise to 4-acetamidobenzenesulfonamide **2** in high conversion with traces of the sulfonic acid **3** (Figure 2a). A model reaction of 9-azidobenzoic acid **6** (10 μM in PBS) under X-ray irradiation afforded 4-aminobenzoic acid **7** although with a conversion <10% (Figure 2e) but excitingly 4-(hydroxymethyl)-2,3,5,6-tetrafluoroaryl azide **4** (10 μM in PBS) was cleanly reduced to 4-(hydroxymethyl)-2,3,5,6-tetrafluoroaniline **5** under X-ray radiation (60 Gy) (Figure 2c). Mechanistically it has been reported that sulfonyl azides can undergo photolysis in alcohols and water via radical mediated chemistry to generate sulphonamides either via a sulfonylamido radical or a nitrene. We suggest a similar mechanism here in which the irradiation source generates hydroxy radicals which react with the sulfonylazide to generate the sulfonylamido radical (and nitrogen), which then abstracts a hydrogen radical from the surrounding environment. An analogous mechanism would likewise operate for the arylazide conversion to the aniline (Figure 2).[32–34]

Activation of fluorescence probe via X-ray irradiation

Following these observations an initial proof-of-concept involved X-ray irradiation unmasking of 7-azido-4-methylcoumarin **8** (Figure 3) to give 7-amino-4-methylcoumarin **9** allowing fluorescence assessment of activation ($\lambda_{ex/em}$ = 345/443 nm, Figure 1b). Conversion of the azide **8** (100 μM in PBS) by irradiation was > 90% with a linear relationship with irradiation dose (Figure 3b and 3c). When HeLa cells were incubated with 7-azido-4-methylcoumarin **8** (100 μM) for 4 h and irradiation applied, flow cytometry (Figure 3e) also showed an increase in fluorescent intensity with increased irradiation dose.

Activation of a pazopanib prodrug

Pazopanib (Votrien®) is an orally available, small-molecule tyrosine kinase inhibitor of the vascular endothelial growth factor (VEGF) receptor 1, 2, and 3.[35,36] Herein, we used pazopanib as one of the models for prodrug activation through X-ray irradiation. The sulfonyl azide prodrug **11** was generated from pazopanib **10** using imidazole-1-sulfonyl azide hydrogen sulfate as the diazotransfer reagent (Figure 4)[37] and its reaction with X-ray irradiation examined. Reaction took place in a radiation dose dependent manner at ambient temperature yielding the drug pazopanib **10** (and the by-product **12**) (Figure 4). The reaction

of prodrug **11** (5 μM. 10 μM and 20 μM in PBS) reached over 90% conversion following X-ray irradiation (60 Gy). Interestingly we observed that the amount of pazopanib **10** increased when irradiation doses increased but reached its highest concentration at 24 Gy (Figure 4) where upon **11** started to decompose, generating the sulfonic acid by-product **12** (Supplementary Fig. 21 and 23). Importantly, pazopanib **10** (20 μM in PBS) remined unreactive under radiation (60 Gy) (Supplementary Fig. 25). To evaluate the efficacy of the combination of radiotherapy and activation of the prodrug, HUVEC were incubated with pazopanib **10** or prodrug **11** (between 5 μM to 20 μM) and irradiated with different doses (from 0 Gy to 60 Gy).[38] We observed that cell viability was both irradiation dose and drug concentration dependent. Activation of prodrug **11** under irradiation generated pazopanib **10** giving significant cell cytotoxicity due to the effect of irradiation and the liberated drug (Figure 4e).

As desired, HUVEC cells treated with prodrug **11** and X-ray irradiation behaved similarly as the pazopanib **10** treated cells, *i.e.* showing lower morbidities, reduced metastasis and tubule formation (see Supplementary Fig. 28, 29 and 30). The successful activation of the caged prodrug molecules was confirmed in an animal model. The successful activation of the caged prodrug molecules was confirmed in an animal model (Figure 4f). Mice treated with the combination of prodrug **11** and X-ray irradiation (purple line) showed comparable efficacy as the drug, with prolonged survival times compared to control groups treated with drug or irradiation individually (Figure 4g).

Activation of a caged doxorubicin prodrug

Based on the model reaction as shown in Figure 2c, where **4** was neatly reduced to a single product **5**, we synthesised (*p*-azido)-2,3,5,6-tetrafluorobenzyloxycarbonyl substituted doxorubicin **13** as an additional prodrug model[39] with another mode of activation, exanimating the reduction of phenyl azide to aniline and subsequent decaging of the drug doxorubicin (Figure 5). Prodrugs **11** and **13** were found to be stable in a broad variety of biological conditions, including whole blood. We observed that the prodrug **13** (10 μM) was also decaged in a radiation dose dependent manner, reaching 50% conversion with 60 Gy (see Figure 5c) with three products (R_T = 4.36, 3.14 and 3.03 min) observed, consisting of doxorubicin **15** (R_T = 3.14 min), tetrafluoroaniline **5 (** R_T = 3.03 min) and the relatively instable “linker-doxorubicin product” **14** (R_T = 4.36 min).[36]

The prodrug was non-toxic when used up to 100 μM, as expected, the IC50 values falls upon irradiation as the active drug is generated (Figure 5d). This drove us to investigate the anticancer efficacy of the prodrug system in animals. Thus in tumour bearing mice model, it was found that tumour growth was significantly inhibited with overall survival prolonged by the combined treatment of X-ray and prodrug **13**. Importantly, evaluations on body weight changes and key organ histological abnormalities (see Figure 5g, Supplementary Figures 42, 43 and 44) showed that the prodrugs displayed no gross toxicities, indeed they reduced the heart toxicity usually found with doxorubicin.[40,41]

Conclusion

We developed a gamma/X-ray mediated strategy for the activation of prodrugs based on the reduction of sulfonyl azide and phenyl azide. The reactions are clearly mediated via free radical chemistry and through the reductive loss of nitrogen,[42] although the exact reductive mechanism is unclear and will be the subject of future studies. For the decaging of doxorubicin from the prodrug, doxorubicin was decaged through a two-step reaction, radical reduction of phenyl azide and 1,6-self-immolation.

The findings here open the way to a whole new area of “ionising irradiation” mediated chemistry – not just for prodrug activation, but for switching on drug delivery from implanted devices, to the generation of a whole suite of tuneable activation chemistries. The local conversion of an inactive prodrug to an active drug via concurrent radiotherapy will lead to much more tolerable treatment regimes without the systemic toxicities observed in conventionally delivered chemotherapies.

Methods

Animals

BALB/c mice and BALB/c nude mice (female, 6-8 week) were provided by Guangdong Medical Laboratory Animal Centre. The housing conditions for the animals were in a barrier environment, with an ambient temperature of 24 °C and a relative humidity of 50%. All the animals were maintained in a 12 h:12 h light–dark cycle. All animal experiments were performed under the Guide for Care and Use of Laboratory Animals and were approved by the Institutional Animal Care and Use Committee (IACUC) of Shenzhen Institutes of Advanced Technology (SIAT).

X-ray source—A linear accelerator (Clinac iX from Varian Medical Systems) generated X-rays of nominal energy 6MV (with a Bremsstrahlung distribution of 2 – 6 MeV) were used, with a dose rate of 600 cGy per minute with samples treated at a depth of 1015 mm from the tungsten target with a build-up of 15 mm of solid water. The linear accelerator used was a Varian Medical Systems VitalBeam medical linear accelerator. The dosage rate of 6 Gy/min was used for all experiments.

Monitoring model reactions under X-ray irradiation

Selected model compounds (see chemical structures in Table 1 and Figure S1) were dissolved in DMSO to give stock solutions of 100 mM and diluted in PBS (20 mL) to give a final concentration of 10 μM. When the solutions were degassed this was done by bubbling Ar for 30 min, followed by X-ray irradiation (0 to 60 Gy, 0 to 10 min). The reaction mixtures after irradiation were analysed by HPLC.

Reaction of coumarin azide 8 under X-ray irradiation

A stock solution of coumarin azide **8** (1 M in DMSO) was diluted in PBS (20 mL) to a final concentration of 100 μM. The solution was degassed by bubbling Ar for 30 min before X-Ray irradiation (0 to 60 Gy). The fluorescence intensity of the reaction mixtures was

analysed. The product **9** was isolated by prep-HPLC and characterised by ^{1}HNMR and HRMS.

Reaction of coumarin azide 8 in live cells under X-ray irradiation

Hela cells were seeded in 24-well plates at a density of 5×10^4 cells per well and incubated overnight. The cells were then treated with coumarin azide **8** (100 μM) 1 h prior to irradiation (0, 6, 36 and 60 Gy) and analysed by flow cytometry using a DAPI filter ($\lambda_{ex/em}$ = 360/450 nm) and confocal microscopy.

Reaction of prodrug 11 under X-ray irradiation

A stock solution of prodrug **11** (100 mM in DMSO) was diluted in PBS (20 mL) to a final concentration of 20 μM. The solution was degassed by bubbling Ar for 30 min before X-Ray irradiation (0 to 60 Gy). The reaction mixture was analysed by FTIR and the products **10** and **12** were isolated by prep-HPLC and characterised ^{1}H-NMR and HRMS.

Reaction of prodrug 13 under X-ray irradiation

A stock solution of doxorubicin prodrug **13** (100 mM in DMSO) was diluted in PBS (20 mL, with 0.1%, *v*/*v* Triton X100) to give a final concentration of 20 μM. The solution was degassed by bubbling Ar for 30 min before X-Ray irradiation (0 to 60 Gy). The reaction mixture was analysed by FTIR and the products **15** and **5** were isolated by prep-HPLC and characterised ^{1}H-NMR and HRMS. (Note compound **15** and **5** co-eluted on the HPLC).

Cell viability against prodrug 13 before and after X-ray irradiation

HeLa cell viability was evaluated using an MTT assay as described above. The cells were treated with prodrug **13** (0.5, 1, 5 and 10 μM) for 4 h, and irradiated with X-ray at 0 Gy, 6 Gy, 12 Gy, 24 Gy, 36 Gy, 48 Gy and 60 Gy. Cells treated with 50% DMSO in DMEM were used as a negative control.

Statistical analysis

Data were presented as mean ± SD. Dunnett's t-tests were used to determine whether the variance between two groups is similar. One-way analysis of variance (ANOVA) was applied for comparison of multiple groups. Statistical analysis was performed using GraphPad Prism. A "P" value < 0.05 was considered statistically significance.

Supplementary Material

Refer to Web version on PubMed Central for supplementary material.

Acknowledgements

We thank the ERC (ERC-2013-ADG 340469 ADREEM) for funding M.B., J.G., K.N. and Y.Z. J.G. acknowledges the support from National Natural Science Foundation of China (22071263), Natural Science Foundation of Guangdong Province, China (2020A1515010994), Guangdong Province Zhujiang Talents Program (2019QN01Y127), Shenzhen Fundamental Research Program (JCYJ20200109110215774) and "Hundred Talents Program" of the Chinese Academy of Sciences. Y.C. acknowledges the support from National Natural Science Foundation of China (22001261) and the China Postdoctoral Science Foundation (2020M672873). Q.G. acknowledges the support from the China Postdoctoral Science Foundation (2020M682976).

Europe PMC Funders Author Manuscripts

Data availability

All relevant data supporting the findings of this study are available within the paper and its Supplementary Information files.

References

(1). Rautio J, Kumpulainen H, Heimbach T, Oliyai R, Oh D, Jarvinen T, Savolainen J. Prodrugs: Design and Clinical Applications. Nat Rev Drug Discov. 2008; 7:255–270. [PubMed: 18219308]

(2). Miwa M, Ura M, Nishida M, Sawada N, Ishikawa T, Mori K, Shimma N, Umeda I, Ishitsuka H. Design of a Novel Oral Fluoropyrimidine Carbamate, Capecitabine, which Generates 5-Fluorouracil Selectively in Tumours by Enzymes Concentrated in Human Liver and Cancer Tissue.[1] . Eur J Cancer. 1998; 34:1274–1281. [PubMed: 9849491]

(3). Krasnovskaya OO, Malinnikov VM, Dashkova NS, Gerasimov VM, Grishina IV, Kireev II, Lavrushkina SV, Panchenko PA, Zakharko MA, Ignatov PA, et al. Thiourea Modified Doxorubicin: a Perspective pH-Sensitive Prodrug. Bioconjugate Chem. 2019; 30:741–750.

(4). Ohwada J, Ozawa S, Kohchi M, Fukuda H, Murasaki C, Suda H, Murata T, Niizuma S, Tsukazaki M, Ori K, et al. Synthesis and Biological Activities of a pH-Dependently Activated Water-Soluble Prodrug of a Novel Hexacyclic Camptothecin Analog. Bioorg Med Chem Lett. 2009; 19:2772–2776. [PubMed: 19362835]

(5). Swift LP, Cutts SM, Rephaeli A, Nudelman A, Phillips DR. Activation of Adriamycin by the pH-Dependent Formaldehyde-Releasing Prodrug Hexamethylenetetramine. Mol Cancer Ther. 2003; 2:189–198. [PubMed: 12589036]

(6). Bentebibel S-E, Hurwitz ME, Bernatchez C, Haymaker C, Hudgens CW, Kluger HM, Tetzlaff MT, Tagliaferri MA, Zalevsky J, Hoch U, et al. A First-in-Human Study and Biomarker Analysis of NKTR-214, a Novel IL2Rβγ-Biased Cytokine, in Patients with Advanced or Metastatic Solid Tumors. Cancer Discov. 2019; 9:711–721. [PubMed: 30988166]

(7). Mustafa AA, Rajan R, Suarez JD, Alzghari SK. A Review of the Opioid Analgesic Benzhydrocodone-Acetaminophen. Cureus. 2018; 10 e2844 [PubMed: 30140595]

(8). Charych D, Khalili S, Dixit V, Kirk P, Chang T, Langowski J, Rubas W, Doberstein SK, Eldon M, Hoch U, et al. Modeling the Receptor Pharmacology, Pharmacokinetics, and Pharmacodynamics of NKTR-214, a Kinetically-Controlled Interleukin-2 (IL2) Receptor Agonist for Cancer Immunotherapy. PLoS ONE. 2017; 12 e0179431 [PubMed: 28678791]

(9). Norman DJ, González-Fernández E, Clavadetscher J, Tucker L, Staderini M, Mount AR, Murray AF, Bradley M. Electrodrugs: an Electrochemical Prodrug Activation Strategy. Chem Comm. 2018; 54:9242–9245. [PubMed: 30066701]

(10). Bezagu M, Clarhaut J, Renoux B, Monti F, Tanter M, Tabeling P, Cossy J, Couture O, Papot S, Arseniyadis S. In Situ Targeted Activation of an Anticancer Agent Using Ultrasound-Triggered Release of Composite Droplets. Eur J Med Chem. 2017; 142:2–7. [PubMed: 28416362]

(11). Hossion AML, Bio M, Nkepang G, Awuah SG, You Y. Visible Light Controlled Release of Anticancer Drug Through Double Activation of Prodrug. ACS Med Chem Lett. 2012; 4:124–127. [PubMed: 24900573]

(12). Sauer R, Becker H, Hohenberger W, Rödel C, Wittekind C, Fietkau R, Martus P, Tschmelitsch J, Hager E, Hess CF, et al. Preoperative Versus Postoperative Chemoradiotherapy for Rectal Cancer. N Engl J Med. 2004; 351:1731–1740. [PubMed: 15496622]

(13). Rosenzweig KE, Gomez JE. Concurrent Chemotherapy and Radiation Therapy for Inoperable Locally Advanced Non–Small-Cell Lung Cancer. J Clin Oncol. 2017; 35:6–10. [PubMed: 27870565]

(14). Alvarado-Miranda A, Arrieta O, Gamboa-Vignolle C, Saavedra-Perez D, Morales-Barrera R, Bargallo-Rocha E, Zinser-Sierra J, Perez-Sanchez V, Ramirez-Ugalde T, Lara-Medina F. Concurrent Chemo-Radiotherapy Following Neoadjuvant Chemotherapy in Locally Advanced Breast Cancer. Radiat Oncol. 2009; 4:24–28. [PubMed: 19591689]

(15). Mao X, McManaway S, Jaiswal JK, Patel PB, Wilson WR, Hicks KO, Bogle G. An Agent-Based Model for Drug-Radiation Interactions in the Tumour Microenvironment: Hypoxia-Activated

Prodrug SN30000 in Multicellular Tumour Spheroids. PLoS Comput Biol. 2018; 14 e1006469 [PubMed: 30356233]

(16). Takakusagi Y, Kishimoto S, Naz S, Matsumoto S, Saito K, Hart CP, Mitchell JB, Krishna MC. Radiotherapy Synergizes with the Hypoxia-Activated Prodrug Evofosfamide: in Vitro and in Vivo Studies. Antioxid Redox Sign. 2018; 28:131–140.

(17). Nytko KJ, Grgic I, Bender S, Ott J, Guckenberger M, Riesterer O, Pruschy M. The Hypoxia-Activated Prodrug Evofosfamide in Combination with Multiple Regimens of Radiotherapy. Oncotarget. 2017; 8

(18). Karzmark CJ. Advances in linear accelerator design for radiotherapy, Advances in Linear Accelerator Design for Radiotherapy. Med Phys. 1984; 11:105–128. [PubMed: 6427568]

(19). Wroe LM, Ige TA, Asogwa OC, Aruah SC, Grover S, Makufa R, Fitz-Gibbon M, Sheehy SL. Comparative Analysis of Radiotherapy Linear Accelerator Downtime and Failure Modes in the UK, Nigeria and Botswana. Clin Oncol. 2020; 32 e111

(20). Shtarkman IN, Gudkov SV, Chernikov AV, Bruskov VI. X-Ray- and Heat-Induced Generation of Hydrogen Peroxide and Hydroxyl Radicals in Aqueous Solutions of L-Amino Acids. Biophysics. 2008; 53:1–7.

(21). Riley PA. Free Radicals in Biology: Oxidative Stress and the Effects of Ionizing Radiation. International Journal of Radiation Biology. 2009; 65:27–33.

(22). Sutherland BM, Bennett PV, Sutherland JC, Laval J. Clustered DNA Damages Induced by X Rays in Human Cells. Radiat Res. 2002; 157:611–616. [PubMed: 12005538]

(23). Sutherland BM, Bennett PV, Sidorkina O, Laval J. Clustered DNA Damages Induced in Isolated DNA and in Human Cells by Low Doses of Ionizing Radiation. Proc Natl Acad Sci USA. 2000; 97:103–108. [PubMed: 10618378]

(24). Lomax ME, Folkes LK, O'Neill P. Biological Consequences of Radiation-Induced DNA Damage: Relevance to Radiotherapy. Clin Oncol. 2013; 25:578–585.

(25). Valerie K, Yacoub A, Hagan MP, Curiel DT, Fisher PB, Grant S, Dent P. Radiation-Induced Cell Signaling: Inside-Out and Outside-in. Mol Cancer Ther. 2007; 6:789–801. [PubMed: 17363476]

(26). Sahin E, Colla S, Liesa M, Moslehi J, Müller FL, Guo M, Cooper M, Kotton D, Fabian AJ, Walkey C, et al. Telomere Dysfunction Induces Metabolic and Mitochondrial Compromise. Nature. 2011; 470:359–365. [PubMed: 21307849]

(27). O'Neill P, Wardman P. Radiation Chemistry Comes Before Radiation Biology. Int J Radiat Biol. 2009; 85:9–25. [PubMed: 19205982]

(28). Azzam EI, Jay-Gerin J-P, Pain D. Ionizing Radiation-Induced Metabolic Oxidative Stress and Prolonged Cell Injury. Cancer Lett. 2012; 327:48–60. [PubMed: 22182453]

(29). Nordsmark M, Bentzen SM, Rudat V, Brizel D, Lartigau E, Stadler P, Becker A, Adam M, Molls M, Dunst J, et al. Prognostic Value of Tumor Oxygenation in 397 Head and Neck Tumors After Primary Radiation Therapy. an International Multi-Center Study. Radiother Oncol. 2005; 77:18–24. [PubMed: 16098619]

(30). Kuzmin GN, Knatko MV, Kurganov SV. Light and X-Ray-Induced Chemistry of Methane on TiO_2 . React Kinet Catal Lett. 1983; 23:313–317.

(31). Barner-Kowollik C, Vana P, Quinn JF, Davis TP. Long-Lived Intermediates in Reversible Addition-Fragmentation Chain-Transfer (RAFT) Polymerization Generated by g Radiation. J Polym Sci Pol Chem. 2002; 40:1058–1063.

(32). Yang Y, Deng G, Lu Y, Liu Q, Abe M, Zeng X. Photodecomposition of Thienylsulfonyl Azides: Generation and Spectroscopic Characterization of Triplet Thienylsulfonyl Nitrenes and 3-Thienylnitrene. J Phys Chem A. 2019; 123:9311–9320. [PubMed: 31593628]

(33). Reagan MT, Nickon A. The Photolysis of Sulfonyl Azides in Isopropyl Alcohol. J Am Chem Soc. 1968; 90:4096–4105.

(34). Dermer OC, Edmison MT. Orientation in Aromatic Substitution by the Benzenesulfonimido Radical. J Am Chem Soc. 1955; 77:70–73.

(35). Bukowski RM, Yasothan U, Kirkpatrick P. Pazopanib. Nat Rev Drug Discov. 2010; 9:17–18. [PubMed: 20043026]

(36). Sleijfer S, Ray-Coquard I, Papai Z, Le Cesne A, Scurr M, Schöffski P, Collin F, Pandite L, Marreaud S, De Brauwer A, et al. Pazopanib, a Multikinase Angiogenesis Inhibitor, in Patients

with Relapsed or Refractory Advanced Soft Tissue Sarcoma: a Phase II Study From the European Organisation for Research and Treatment of Cancer–Soft Tissue and Bone Sarcoma Group (EORTC Study 62043). J Clin Oncol. 2009; 27:3126–3132. [PubMed: 19451427]

(37). Stevens MY, Sawant RT, Odell LR. Synthesis of Sulfonyl Azides via Diazotransfer Using an Imidazole-1-Sulfonyl Azide Salt: Scope and 15N NMR Labeling Experiments. J Org Chem. 2014; 79:4826–4831. [PubMed: 24802878]

(38). Zhu X-D, Zhang J-B, Fan P-L, Xiong Y-Q, Zhuang P-Y, Zhang W, Xu H-X, Gao D-M, Kong L-Q, Wang L, et al. Antiangiogenic Effects of Pazopanib in Xenograft Hepatocellular Carcinoma Models: Evaluation by Quantitative Contrast-Enhanced Ultrasonography. BMC Cancer. 2011; 11:307. [PubMed: 21781302]

(39). Matikonda SS, Fairhall JM, Fiedler F, Sanhajariya S, Tucker RAJ, Hook S, Garden AL, Gamble AB. Mechanistic Evaluation of Bioorthogonal Decaging with Trans-Cyclooctene: the Effect of Fluorine Substituents on Aryl Azide Reactivity and Decaging From the 1,2,3-Triazoline. Bioconjugate Chem. 2018; 29:324–334.

(40). Doroshow JH. Effect of Anthracycline Antibiotics on Oxygen Radical Formation in Rat Heart. Cancer Res. 1983; 43:460–472. [PubMed: 6293697]

(41). Olson RD, Mushlin PS. Doxorubicin Cardiotoxicity: Analysis of Prevailing Hypotheses. FASEB J. 1990; 4:3076–3086. [PubMed: 2210154]

(42). Benati L, Bencivenni G, Leardini R, Minozzi M, Nanni D, Scialpi R, Spagnolo P, Zanardi G. Radical Reduction of Aromatic Azides to Amines with Triethylsilane. J Org Chem. 2006; 71:5822–5825. [PubMed: 16839176]

Europe PMC Funders Author Manuscripts

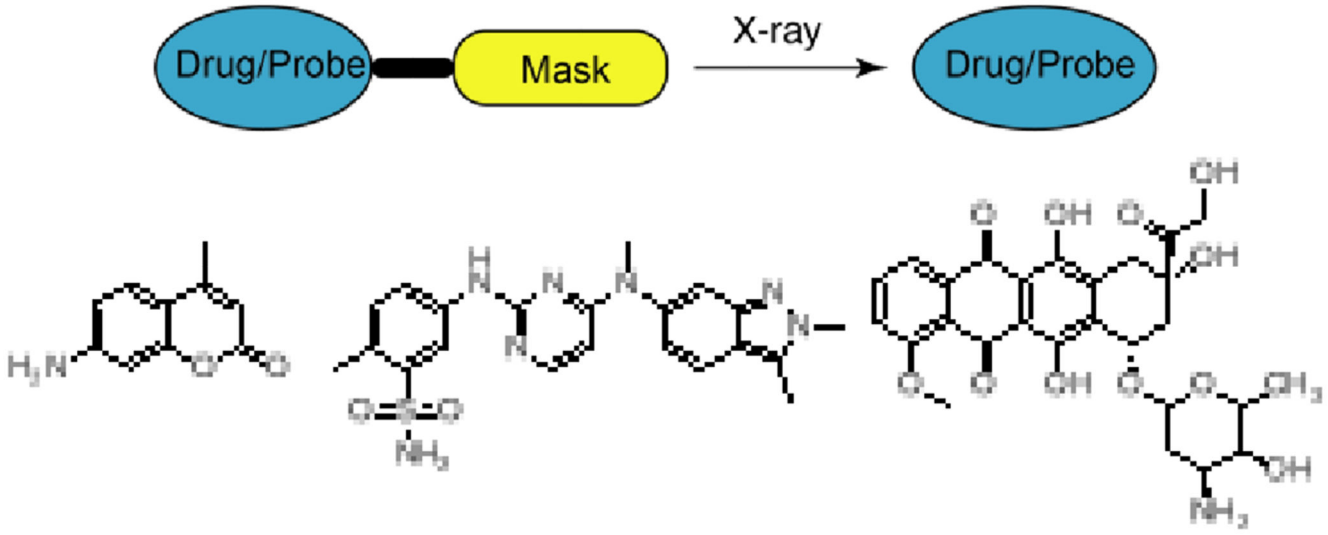

Figure 1.
Drug/probe decaging via X-ray irradiation. Coumarin was used as a probe model, and pazopanib and doxorubicin were used as anticancer agents.

Europe PMC Funders Author Manuscripts

Europe PMC Funders Author Manuscripts

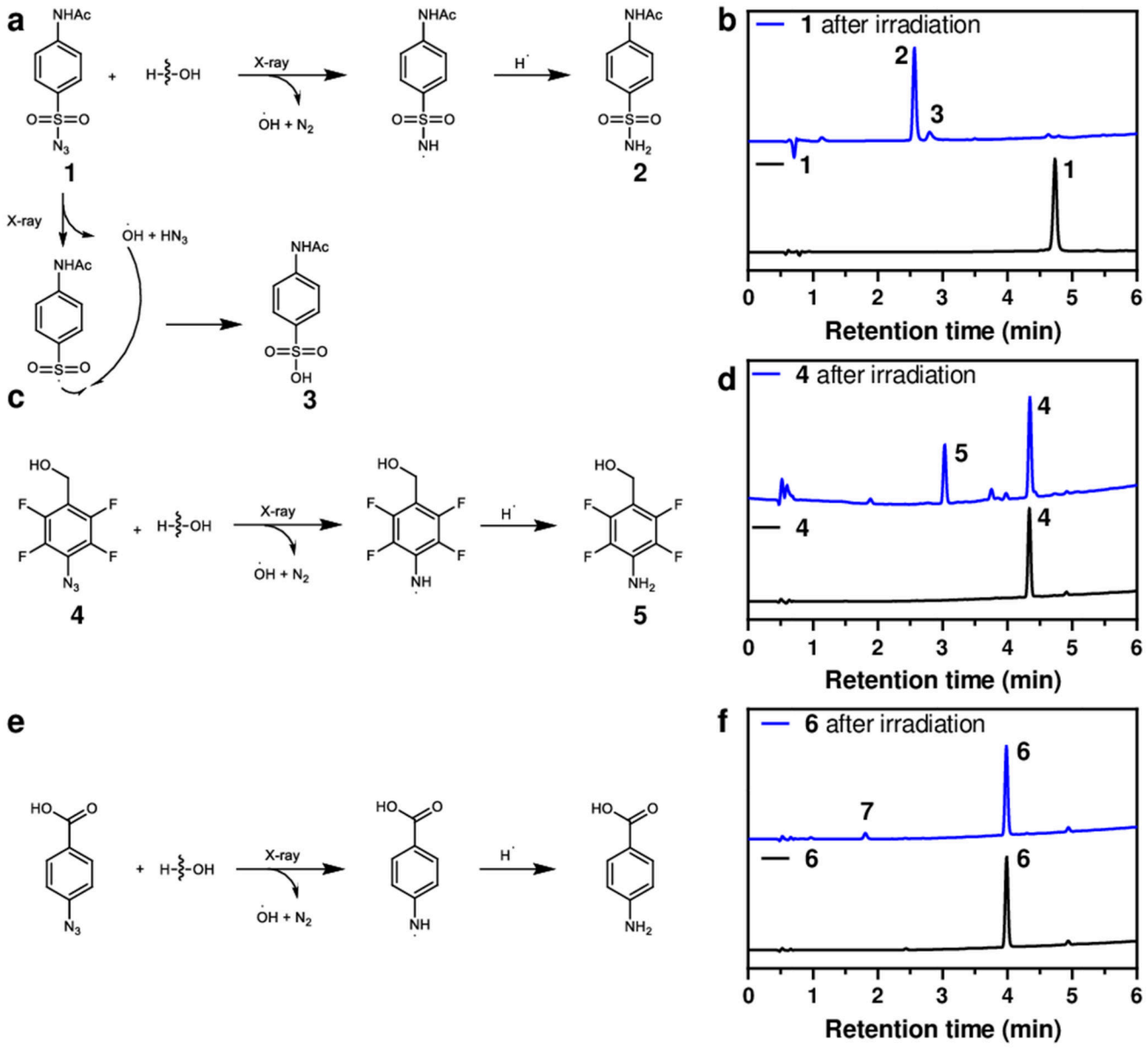

Figure 2. Model reaction of 1, 4 and 6 under X-ray irradiation.

(**a**) Mechanism of reaction of 4-acetamidobenzenesulfonyl azide **1** under X-ray irradiation. (**b**) HPLC traces of **1** upon irradiation (20 μM, 60 Gy, 6 Gy/min) that afforded **2** (R_T = 2.61 min) and **3** (R_T = 2.83 min) with a full conversion of **1** (R_T = 4.89 min). (**c**) Mechanism of reaction of 4-(hydroxymethyl)-2,3,5,6-tetrafluoroaryl azide **4** under X-ray irradiation that resulted in the generation of 4-(hydroxymethyl)-2,3,5,6-tetrafluoroaniline **5**. (**d**) HPLC traces of **4** (R_T = 4.31 min) upon irradiation (20 μM, 60 Gy, 6 Gy/min) that afforded **5** (R_T = 3.01 min). (**e**) Mechanism of reaction of 4-azidobenzoic acid **6** under X-ray irradiation. (**f**) HPLC traces of **6** (R_T = 3.99 min) and irradiated **6** (20 μM, 60 Gy, 6 Gy/min) that afforded poor conversion to 4-aminobenzoic acid **7** (R_T = 1.79 min). HPLC chromatogram showing UV absorbance at 254 nm.

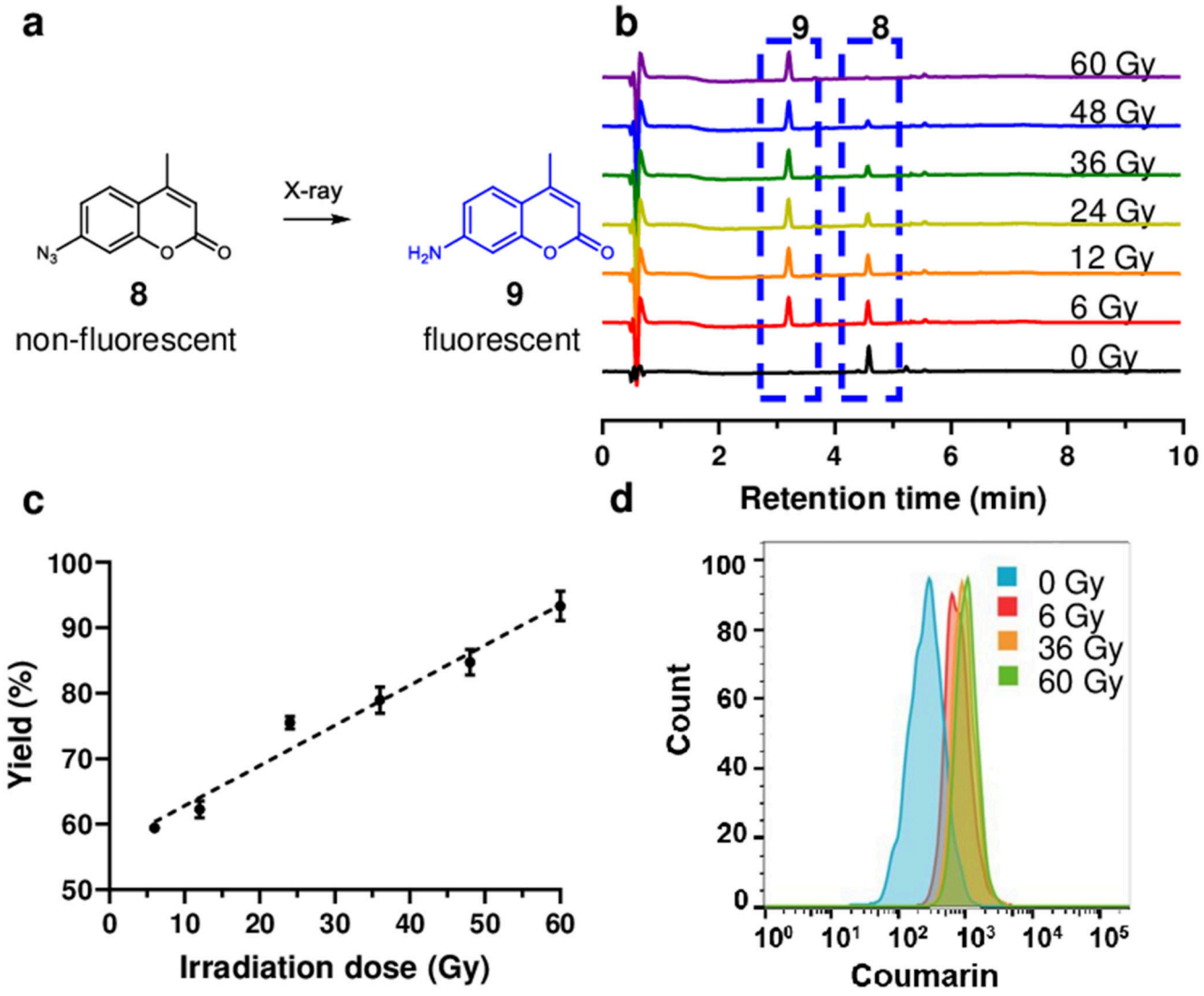

Figure 3. X-ray irradiation mediated activation of azido coumarin.

(**a**) Irradiation of 7-azido-4-methylcoumarin **8** resulting in the generation of 7-amino-4-methylcoumarin **9** with fluorescence turn-on. (**b**) HPLC traces of the reaction mixture of **8** (R_T = 4.57 min) after irradiation with 0 Gy to 60 Gy to afforded product **9** (R_T = 3.21 min). (**c**) Graph showing the yield of **9** generated with different irradiation doses. The data are presented as mean ± SD (n = 3). (**d**) Flow cytometry analysis ($\lambda_{ex/em}$ = 360/450 nm) of cells incubated with **8** (100 μM) with **9** generated in cells following 0 Gy, 6 Gy, 36 Gy and 60 Gy irradiation. Forward versus side scatter profiles were used to gate intact cellular materials. Flow cytometry analyses are based on a population of 10,000 cells.

Europe PMC Funders Author Manuscripts

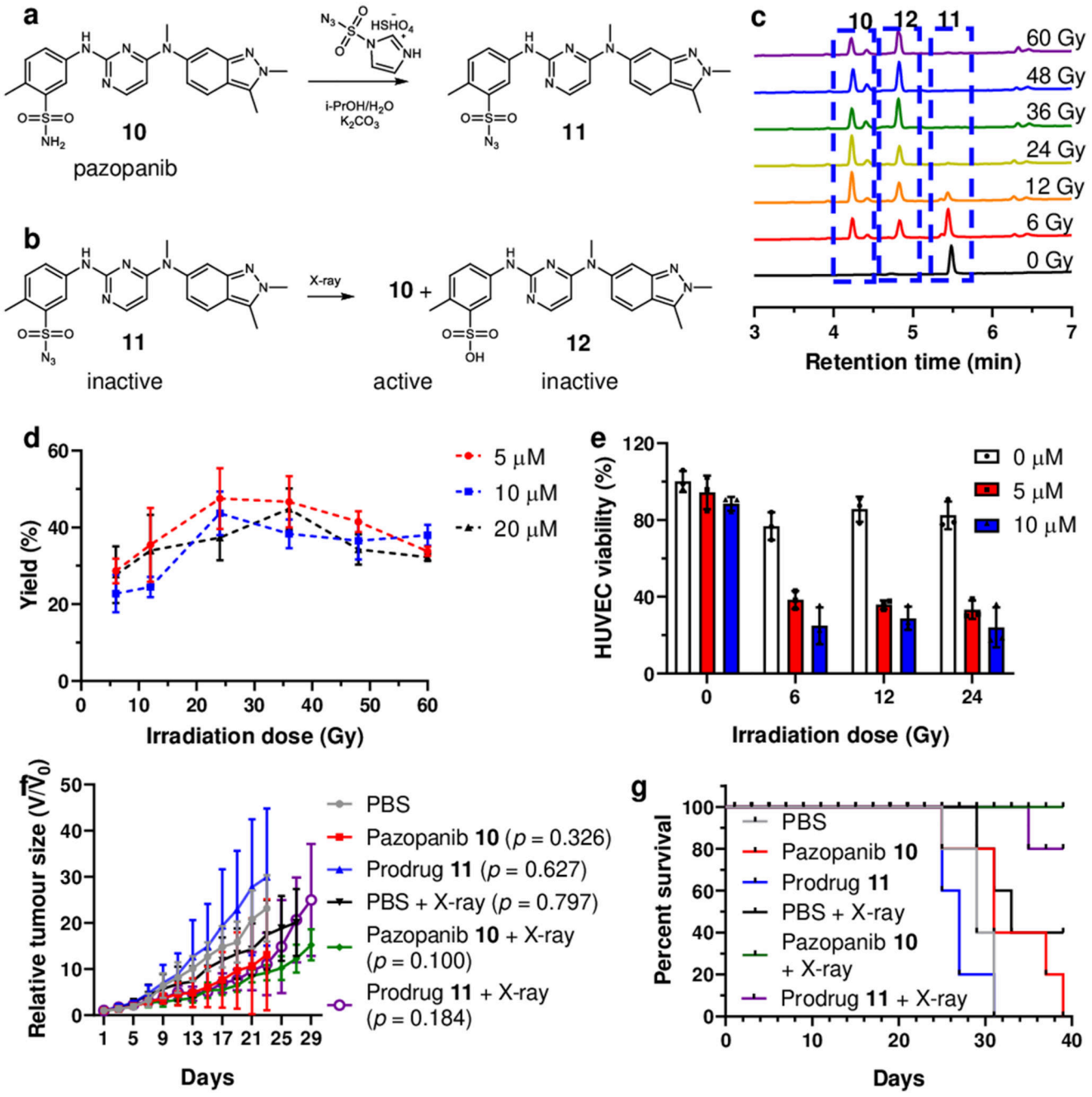

Figure 4. Synthesis of the pazopanib prodrug 11 and analysis of the irradiation reaction *in vivo*.

(**a**) Synthesis of prodrug **11** from pazopanib (**10**, 83 mM) in H_2O/*i*-PrOH with imidazole-1-sulfonyl azide (1.5 equiv.) and K_2CO_3 (4 equiv.), 18 h, yield 65%. (**b**) The reaction of prodrug **11** under irradiation afforded products, **10** (pazobanib) and **12**. (**c**) HPLC traces of the reaction mixture of prodrug **11** (R_T = 5.44 min) after irradiation (0 Gy to 60 Gy) to afford product **10** (R_T = 4.23 min) and **12** (R_T = 4.83 min) with some remaining unreacted prodrug **11**. (**d**) The yield of pazopanib **10** generated from prodrug **11** (5, 10 and 20 μM) under irradiation from 6 Gy up to 60 Gy (6 Gy/min). The data are presented as mean ± SD

(n = 3). (**e**) HUVEC viability upon treatment of prodrug **11** (0, 5 and 10 μM) and X-ray irradiation (0, 6, 12 and 24 Gy). The data are presented as mean ± SD (n = 3) (**f**) HT-29 tumour bearing BALB/c nude mice were treated with prodrug **11** by intratumoural injection. 4 h post injections, mice were treated with or without 6 Gy of X-ray irradiation. Tumour burdens were measured every other day using a calliper. The data are presented as mean ± SD (n = 5). Statistical analysis was performed using one-way ANOVA with Dunnett post-test compared to PBS treated mice at day 23. (**g**) Survival curves for HT29 tumour bearing mice. Mice were aged until moribund or the tumour volume reached 2000mm^3 (n = 5).

Europe PMC Funders Author Manuscripts

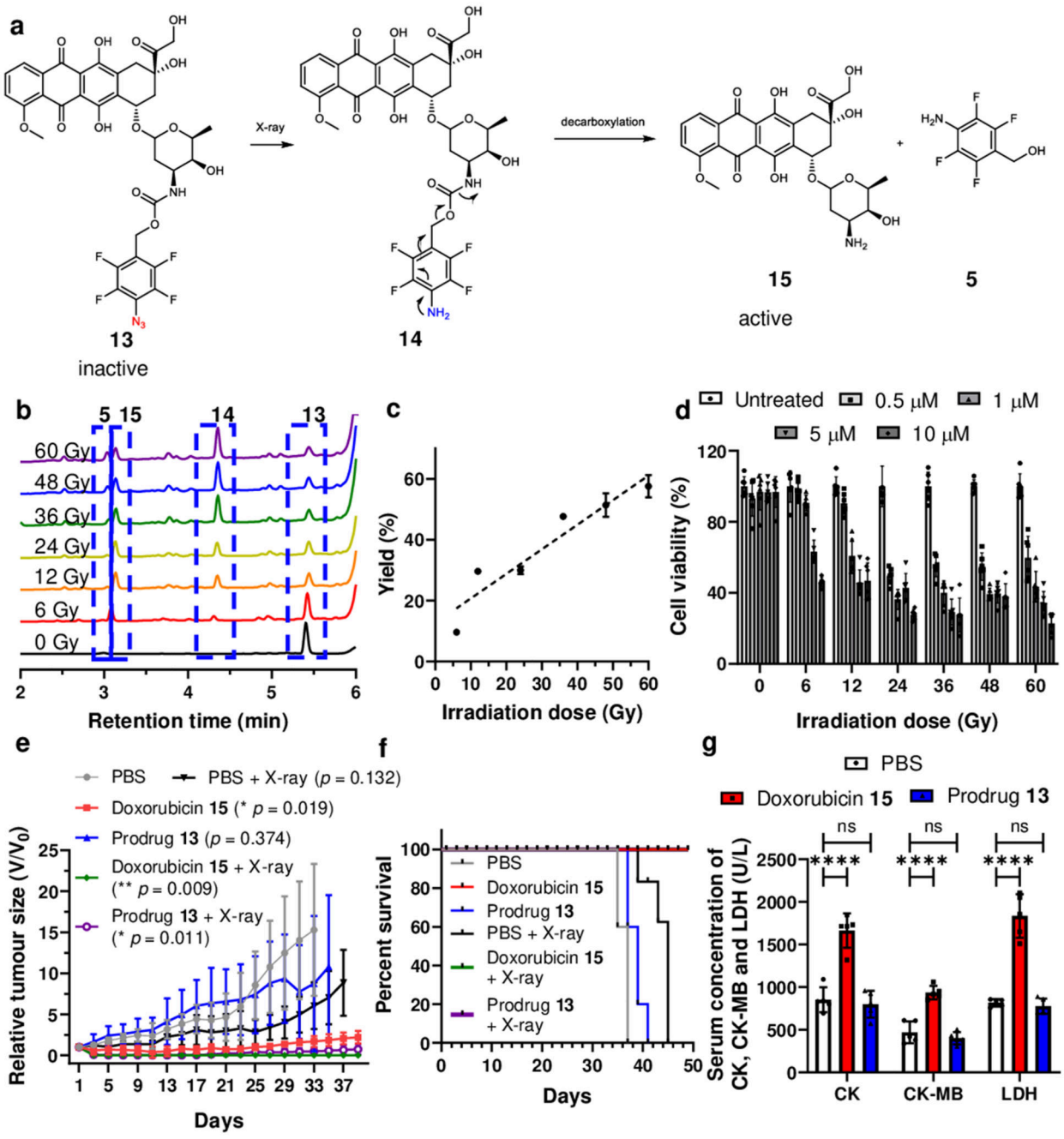

Figure 5. Doxorubicin prodrug activation by X-ray irradiation.

(**a**) The reaction of the doxorubicin prodrug **13** and mechanistic pathway for liberation of doxorubicin, **15**. (**b**) HPLC traces of the reaction mixture of prodrug **13** after irradiation with 0 Gy to 60 Gy, showing unreacted prodrug prodrug **13** (R_T = 5.40 min), intermediate **14** (R_T = 4.36 min), doxorubicin **15** (R_T = 3.14 min) and **5** (R_T = 3.03 min). (**c**) The yield of doxorubicin **15** generated from prodrug **13** (10 μM) under irradiation (6 Gy up to 60 Gy, 6 Gy/min). Due to the poor solubility of doxorubicin the irradiation mixture was extracted into an organic solvent prior to HPLC analysis. The data are presented as mean ± SD (n = 3). (**d**)

Europe PMC Funders Author Manuscripts

Europe PMC Funders Author Manuscripts

HeLa cells were incubated with prodrug **13** (0.5, 1, 5 and 10 μM) for 4 h, followed by X-ray irradiation (from 0 Gy to 60 Gy) and cell viability measured using an MTT assay after 24 h incubation at 37 °C. The data are presented as mean ± SD (n = 6). (**e**) HeLa tumour bearing BALB/c nude mice were treated with prodrug **13** by intratumoural injection. 4 h post injections, mice were treated with or without 6 Gy of X-ray irradiation. Tumour burdens were measured every other day using a calliper. The data are presented as mean ± SD (n = 5). Statistical analysis was performed using one-way ANOVA with Dunnett post-test compared to PBS treated mice at day 33. (**f**) Survival curves for HT29 tumour bearing mice. Mice were aged until moribund or the tumour volume reached 2000mm^3. (n = 5), (**g**) Biochemical markers CK, CK-MB and LDH levels in plasma 48 h after PBS, prodrug **13** and doxorubicin **15** treatments. The data are presented as mean ± SD (n = 5). Statistical analysis was performed using one-way ANOVA with Dunnett post-test compared to PBS treated mice, **** $P < 0.001$, ns (not significant).

Europe PMC Funders Author Manuscripts

Table 1

Model reactions under X-ray Irradiation.[a]

Compound	Reaction[b]	Number of Products[c]	Compound	Reaction[b]	Number of Products[c]
	N	-		N	-
	Y	>2		Y	>5
	N	-		Y	3
	Y	1		Y	1
	N	-		N	-
	N	-		N	-
	Y	1		N	-
	N	-		Y	2

[a] reactions were all carried out in PBS with concentration of 10 μM and under 60 Gy irradiation

[b] N = not reacted, Y = reacted;

[c] confirmed by HPLC chromatography (254 nm).